Negative Full Counting Statistics Arise from Interference Effects

Patrick P. Hofer[1,2] and A. A. Clerk[1]
[1]Department of Physics, McGill University, Montreal, Quebec, Canada H3A 2T8
[2]Département de Physique Théorique, Université de Genève, 1211 Genève, Switzerland
(Received 15 October 2015; published 7 January 2016)

The Keldysh-ordered full counting statistics is a quasiprobability distribution describing the fluctuations of a time-integrated quantum observable. While it is well known that this distribution can fail to be positive, the interpretation and origin of this negativity has been somewhat unclear. Here, we show how the full counting statistics can be tied to trajectories through Hilbert space, and how this directly connects negative quasiprobabilities to an unusual interference effect. Our findings are illustrated with the example of energy fluctuations in a driven bosonic resonator; we discuss how negative quasiprobability here could be detected experimentally using superconducting microwave circuits.

DOI: 10.1103/PhysRevLett.116.013603

Introduction.—Quasiprobability distributions such as the Wigner function [1] are powerful tools that allow one to visualize quantum states in phase space. They have played a seminal role in quantum mechanics since the early beginnings of the theory. Among their many uses are the identification of nonclassical states: these are states where the Wigner function (or some other related distribution) fails to be positive definite (see, e.g., Ref. [2]). Such nonclassicality can constitute a resource for quantum information processing [3,4].

Recently, a very different kind of quasiprobability distribution has found widespread utility, the so-called full counting statistics (FCS) [5–7]. Unlike the Wigner function, the FCS does not describe the instantaneous state of a quantum system, but rather describes its time history and dynamics: it characterizes the fluctuations of a time-integrated quantum observable. As has been discussed extensively, the FCS distribution describes the "intrinsic" fluctuations of the system absent any coupling to a measurement device [7,8]. Nonetheless, it can be used to directly predict the outcome of realistic measurement setups, where the added noise of the measurement combines with the intrinsic system fluctuations to determine the final measured distribution [7–10]. FCS first arose in the study of current fluctuations in quantum electronic conductors, where the transmitted charge is the time integral of the current operator [5,6,11]; it continues to be a crucial tool in quantum transport, and has also been used to characterize cold atom systems [12], work [13] and heat fluctuations [14], dynamical phase transitions of classical systems [15,16], and quantum-optical systems [8]. FCS have also recently been connected to weak measurement theory [9,17].

Similar to conventional quasiprobability distributions, the FCS distribution can fail to be positive definite. As the FCS describes the time history of a system, negativity here is indicative of the presence of nonclassical temporal correlations and/or dynamics which render a backaction-free measurement impossible [8,9]. Largely because many of the most studied systems are immune to backaction (e.g., gauge invariant electronic transport at long times), and thus described by a positive-definite FCS [7], very little work has been undertaken on the meaning, origin, or utility of negative FCS; notable exceptions are Refs. [8–10,18–20]. Considering the utility of negativities in more conventional quasiprobabilities, it is desirable to obtain a better understanding of negative FCS.

In this work we present a clear physical picture for how negative FCS emerge. We connect the FCS distribution to trajectories the system takes through Hilbert space. The resulting expression gives an intuitive understanding of the microscopic processes that contribute to the FCS and allows us to show that negative FCS are the direct result of an unusual interference phenomena: the interference of amplitudes associated with two trajectories can contribute to the quasiprobability, even though the classical probabilities for each trajectory do not contribute. Our approach also demonstrates why negative FCS in general requires systems where a few degrees of freedom are relatively isolated. We stress that, in contrast with Refs. [7,21–23], our main focus is to understand the negativity in the FCS, and not on how the inclusion of detectors modifies the FCS and restores positivity in the final measured distribution. Nonetheless, our approach also gives an intuitive picture of this process [see Supplemental Material [24]]. Our approach is particularly well suited to investigating the short-time FCS, a regime that is relevant to fast experimental protocols but that has received only limited attention.

To make the utility of our approach clear, we focus on a particularly simple system that exhibits negative FCS: the time-integrated energy fluctuations in a coherently driven bosonic single-mode resonator. The FCS here are particularly amenable to experimental measurement, and their negativity was recently discussed as a potentially powerful way to detect nonclassical behavior in an optomechanical system [20]. Finally, we analyze a realistic circuit quantum electrodynamics (cQED) measurement setup for detecting negative FCS.

Definition of FCS.—We consider an observable $\hat{n}(t)$ in the Heisenberg picture, and are interested in characterizing the fluctuations of its time integral $\hat{m} = \int_0^t dt' \hat{n}(t')$. Since $\hat{n}(t)$ does not necessarily commute with itself at different times, the higher moments of $\hat{m}$ will be contingent on how one chooses to time order the various factors of $\hat{n}$. The well-developed field of FCS resolves this ambiguity by considering how one would measure $\hat{m}$; guided by this, the appropriate moment generating function for m is [5–7] ($\hbar = 1$)

$$\Lambda(\lambda) \equiv \int dm P(m) e^{-i\lambda m} \equiv \mathrm{Tr}\{e^{-i\hat{H}_\lambda t} \hat{\rho} e^{i\hat{H}_{-\lambda} t}\}, \quad (1)$$

where $P(m)$ is the quasiprobability distribution of interest (the FCS), $\hat{\rho}$ is the system density matrix at $t = 0$, and $\hat{H}_\lambda = \hat{H} + \lambda\hat{n}/2$, with $\hat{H}$ being the Hamiltonian of the system.

A simple way to motivate Eq. (1) is to consider an idealized measurement where an auxiliary qubit couples to $\hat{n}$ via $\hat{H}_c = \lambda\hat{n}\hat{\sigma}_z/2$ [5]. If $\hat{n}$ were a classical stochastic variable $n(t)$, the qubit would precess by an angle $\lambda m = \lambda \int_0^t dt' n(t')$, and the off-diagonal reduced density matrix element would directly yield the average of $\exp(-i\lambda m)$, i.e., the moment generating function. This then motivates Eq. (1) in the quantum case. This is only one of several idealized measurement schemes that lead to Eq. (1) [7,8,20]. Equation (1) can also be motivated by the Keldysh path-integral approach [25]. The time ordering of $\hat{n}(t)$, which ultimately leads to the negativities in the FCS, is thus dictated by the fact that the FCS is a measurement-independent quantity.

Unravelling the FCS.—In the spirit of Feynman's path-integral approach, we now divide the time evolution in Eq. (1) into N infinitesimal steps of duration δt; between these partitions, we introduce resolved identity operators. We start with the simplest case, where $\hat{n}$ has a discrete spectrum, and further, where our system has no additional quantum numbers, such that $\mathbb{I} = \sum_n |n\rangle\langle n|$ is the identity operator. Inserting the identities allows us to replace the operator $\hat{n}$ by its eigenvalues. The FCS can then be obtained by Fourier transforming Eq. (1),

$$P(m) = \sum_{\vec{n}_L, \vec{n}_R} \delta_{n_f^L, n_f^R} \delta\left(m - \frac{1}{2} m_L - \frac{1}{2} m_R\right) \times \langle n_1^L | \hat{\rho} | n_1^R \rangle A(\vec{n}_L) A^*(\vec{n}_R), \quad (2)$$

with the amplitudes

$$A(\vec{n}_\alpha) = \langle n_f^\alpha | e^{-i\hat{H}\delta t} | n_N^\alpha \rangle \cdots \langle n_2^\alpha | e^{-i\hat{H}\delta t} | n_1^\alpha \rangle. \quad (3)$$

Here the n_j^α denote the states inserted at the jth time slice either on the left ($\alpha = L$) or on the right side of the density matrix ($\alpha = R$) in Eq. (1). The quantity $A(\vec{n}_\alpha)$ gives the amplitude for a trajectory through Hilbert space, defined by the vector $\vec{n}_\alpha = (n_1^\alpha, \ldots, n_N^\alpha, n_f^\alpha)$. The time integral of the observable $\hat{n}$ over such a discrete trajectory is given by $m_\alpha = \sum_j n_j^\alpha \delta t$. Examples of such trajectories are illustrated in Figs. 1(a) and 1(b). Finally, as we are interested in the $\delta t \to 0$ limit, we neglect terms that are order $(\delta t)^2$ and higher.

Each term in Eq. (2) describes the contribution to $P(m)$ from a pair of trajectories $\vec{n}_L$ and $\vec{n}_R$; the second line is the product of probability amplitudes for each of the trajectories, weighted by the density matrix element corresponding to the initial "position" of each trajectory. The trajectories are summed over, given the constraints on the first line. The Kronecker delta enforces the two trajectories to end at the

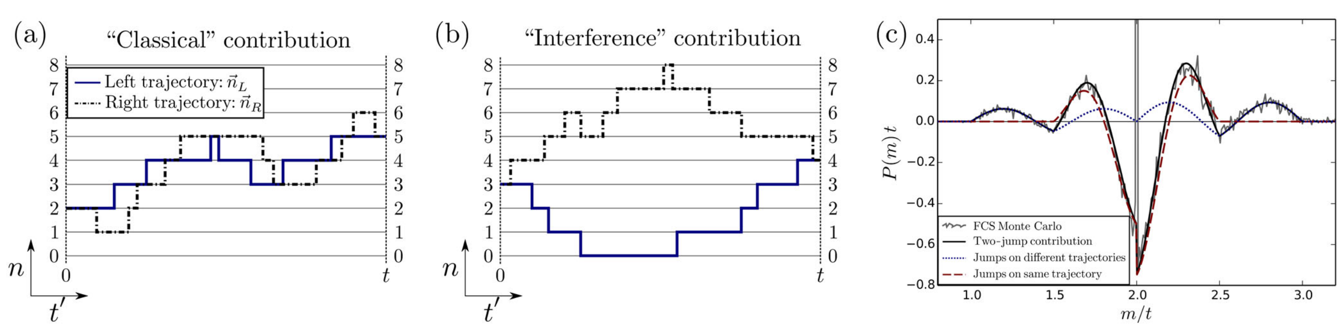

FIG. 1. FCS for a bosonic resonator and contributing pairs of trajectories. (a) Illustration of a pair of trajectories contributing to $P(m_0)$, where the m value of each trajectory is the same: $m_L = m_R = m_0$. Such pairs yield a positive contribution. (b) Illustration of a pair of trajectories with $m_L \neq m_R$, but $(m_L + m_R)/2 = m_0$. As discussed in the text, such a pair can yield a negative contribution to $P(m_0)$. (c) FCS for a cavity initially prepared in the $n_0 = 2$ Fock state. The analytical result (black, solid line) consists of a contribution where the jumps are located on different trajectories (blue, dotted line) and a contribution where the jumps are located on the same trajectory (red, dashed line). The singular, zero-jump contribution of Eq. (5) is omitted. A Monte Carlo simulation (gray line) using 50 000 trajectories is in good agreement with the analytical results. Parameters are time $t = 4/\Delta$, drive strength $f = \Delta/16$, where Δ is the drive detuning.

same position and is a consequence of the trace in Eq. (1). The Dirac delta tells us that a pair of trajectories contributes to $P(m)$ when m is equal to the *average* of m_L and m_R.

While Eq. (2) is just a direct representation of the standard FCS $P(m)$ distribution, we immediately notice a rather strange feature: for a given particular value m_0, the interference terms between two trajectories can contribute to $P(m_0)$ even though the corresponding classical probabilities do not. To be explicit, suppose we have a pair of trajectories with m values m_L and m_R. The classical probability from each trajectory, i.e., the terms proportional to $|A(\vec{n}_L)|^2$ and $|A(\vec{n}_R)|^2$, contribute to $P(m_L)$ and $P(m_R)$, respectively. Their interference terms, i.e., the terms proportional to $A(\vec{n}_L)A^*(\vec{n}_R)$ and $A(\vec{n}_R)A^*(\vec{n}_L)$, contribute instead to $P(m_L/2 + m_R/2)$. If $m_L \neq m_R$, the interference terms are thus separated from their classical probabilities, allowing the quasiprobability distribution $P(m)$ to become negative. We thus have one of the key conclusions of our approach: negativity in the distribution $P(m)$ is directly and necessarily connected to a kind of anomalously strong influence of interferences between pairs of trajectories.

This motivates us to separate the contributions to the sum in Eq. (2) into two generic kinds. Terms with $m_L = m_R$ are denoted “classical” contributions. These yield a total contribution to $P(m)$ that is positive definite. Terms with $m_L \neq m_R$ are denoted “interference” contributions. These are the interference terms that are separated from their classical probabilities and responsible for any negativities in the FCS. Examples of pairs of trajectories yielding classical and interference contributions to $P(m)$ are illustrated in Figs. 1(a) and 1(b).

Driven cavity.—We now illustrate our trajectory approach to FCS by considering a coherently driven bosonic single-mode resonator, first in the absence of any dissipation. This constitutes a simple system that is amenable to cQED [26–28] and optomechanical [29,30] experiments. In the frame rotating at the driving frequency, the Hamiltonian of the system reads

$$\hat{H} = \Delta \hat{a}^\dagger \hat{a} - f(\hat{a}^\dagger + \hat{a}), \tag{4}$$

where Δ denotes the detuning of the drive and f the drive strength (which we take to be real without loss of generality). We are interested in the photon number fluctuations, $\hat{n} = \hat{a}^\dagger \hat{a}$. Despite the seemingly trivial nature of the system and its linear dynamics, we are measuring a nonlinear observable, and the integrated-energy fluctuations are described by negative FCS [8].

The coherent drive can induce jumps in the trajectories (i.e., from one Fock state to another), whereas the detuning introduces a phase factor in $A(\vec{n}_L)A^*(\vec{n}_R)$ whenever $m_L \neq m_R$. For $ft \ll 1$, only pairs of trajectories with a low number of jumps will contribute to the FCS, and we can make some analytical progress. To this end, we consider an initial Fock state $\hat{\rho} = |n_0\rangle\langle n_0|$ and pairs of trajectories including a total of up to two jumps. The contribution from pairs exhibiting no jumps at all is given by

$$P_0(m) = \delta(m - n_0 t). \tag{5}$$

The zero jump contribution thus reflects the initial distribution and does not decay with time. To ensure the normalization of $P(m)$, all contributions with a higher number of jumps must thus average to zero: this ensures negativities in the FCS as long as the dynamics of the system is nontrivial. These considerations remain valid for an arbitrary initial state.

For an initial Fock state, there is no contribution from pairs of trajectories exhibiting a single jump in total because of the Kronecker delta in Eq. (2). The two jump contribution is discussed in the Supplemental Material [24] and plotted in Fig. 1(c) together with a Monte Carlo simulation of the FCS. As illustrated in Fig. 1(c), the distribution $P(m)$ shows a highly nontrivial behavior and becomes negative over a substantial range of its argument. The jump at $m/t = n_0$ as well as the kinks at $m/t = n_0 \pm 1/2$ are a consequence of the discreteness of photon numbers and can be well understood in terms of the few trajectories that contribute at short times (see Supplemental Material [24]).

We stress that these unusual short-time features also occur for different choices of initial states, including a coherent state; in that case, our calculations agree with the approach used in Refs. [8,31] (see also Fig. 2). The presence of negative FCS is thus not a function of the initial state, but rather reflects the nonclassicality of the system dynamics; this is in stark contrast to the Wigner function (where coherent states exhibit no negativity). We thus conclude that even systems that remain in a seemingly near-classical state at all times can exhibit extremely nonclassical behavior in their dynamics.

Additional degrees of freedom.—Equation (2) (and the single resonator example) discussed so far are somewhat special cases, in that the relevant dynamics only involves a single degree of freedom. As we now show, if the dynamics starts to couple to additional degrees of freedom, negativity can be rapidly lost, as there is a strong suppression of the required “interference” contributions.

Consider first the situation where the additional degrees of freedom correspond to a dissipative environment; for concreteness, we return to our example of a driven resonator, and add a coupling to a Markovian bath. In such a situation, the contribution of the bath to the dynamics can be modeled in terms of dissipative quantum jumps, in complete analogy to how they are treated in the standard quantum trajectory approach of quantum optics [32]. These dissipation-induced jumps are described by the superoperators

$$\mathcal{J}_\downarrow \hat{\rho} = \kappa(n_B + 1)\hat{a}\,\hat{\rho}\,\hat{a}^\dagger, \qquad \mathcal{J}_\uparrow \hat{\rho} = \kappa n_B \hat{a}^\dagger \hat{\rho}\,\hat{a}, \tag{6}$$

where κ is the energy damping rate and n_B is the thermal occupation number of the bath at the cavity frequency. The first (second) term describes photons that are lost to (gained from) the bath.

We can again incorporate these jump operators into a path-integral expression for the FCS distribution function

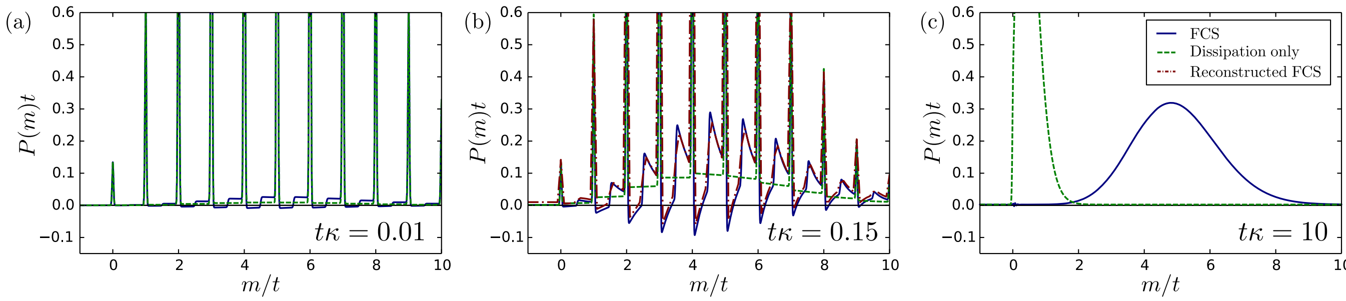

FIG. 2. Time evolution of the integrated-energy FCS for a damped cavity initially prepared in a coherent state. The blue curve shows the FCS in the presence of a coherent drive with strength $f/\kappa = \sqrt{5}/2$, where κ is the energy damping rate. The green curve shows the FCS describing the dissipative emptying of the cavity ($f = 0$). The resulting distribution is fully positive and can be described with a classical model. (a) At very short times, the FCS is dominated by peaks at integer m/t reflecting the initial photon distribution. (b) The exchange of photons with the coherent drive and the dissipative bath leads to features in between the peaks which can be understood in terms of the few-jump trajectories. An experimental reconstruction of the FCS (red, dash-dotted line) using an auxiliary qubit detector is feasible using 500 measurements covering a range of λ up to $\lambda_{\max} = 418.9\kappa$ (see main text). (c) At long times, the FCS is a continuous function peaked around the mean photon number in the cavity. Except for the reconstructed FCS, all distributions are convolved with a sharply peaked Gaussian (width $\sigma = t\kappa/10$) to resolve the Dirac deltas. For all panels, the drive is on resonance $\Delta = 0$.

$P(m)$; see Supplemental Material [24]. Similar to standard quantum trajectory theory, the dissipation correlates the behavior of the left and right trajectories, thus suppressing the negativity-induced interference contributions (which require distinct trajectories on the left and on the right). For a purely dissipative process, the left and the right trajectories are always identical and the FCS always positive, being a simple sum of classical probabilities. In this case, the FCS recovers the results obtained by classical master equations (see Fig. 2). Details on the dissipative FCS calculation are provided in the Supplemental Material [24] along with a discussion on how coupling coherently to an additional degree of freedom also suppresses negativity.

Time evolution of the FCS.—To stress the utility of our approach we consider the time evolution of the FCS in an experimentally relevant system. To this end, we add dissipation to our driven cavity system resulting in the Lindblad master equation

$$\frac{d\hat{\rho}}{dt} = -i[\hat{H}, \hat{\rho}] - \frac{\kappa}{2}\{\hat{a}^\dagger \hat{a}, \hat{\rho}\} + \kappa \hat{a}\,\hat{\rho}\,\hat{a}^\dagger, \tag{7}$$

where $\hat{H}$ is given in Eq. (4). As an initial state, we take the steady-state solution which is given by a coherent state with an average photon number, $n_D = 4f^2/(\kappa^2 + 4\Delta^2)$. Since in this case the Wigner function is Gaussian at all times, we use the method described in detail in Refs. [8,31] to calculate the moment generating function. The time evolution of the resulting FCS is illustrated in Fig. 2. At very short times [cf. Fig. 2(a)], the FCS is dominated by sharp peaks at integer m/t corresponding to trajectories where the photon number remains constant. At large times [cf. Fig. 2(c)], the FCS is a smooth function centered around the mean photon number n_D. At times where the trajectories with few jumps dominate [cf. Fig. 2(b)], the FCS exhibits features in between the peaks at integer m/t. For a purely dissipative process, the FCS is continuous in between the peaks and can be captured by a classical calculation involving only occupation probabilities. In the presence of a coherent drive, the FCS exhibits a surprising shape with discontinuities at half-integer m/t. In complete analogy to Fig. 1(c), this can be well understood in terms of the few-jump trajectories and ultimately results from the discreteness of the number of photons. The jumps at half-integer m/t are a consequence of the coherences in the initial state. Our approach thus allows for a quantitative understanding of the nontrivial short-time FCS.

Reconstructing the FCS.—As discussed in detail in the Supplemental Material [24], measurement noise (uncertainty and backaction) will often mask the sharp features that are characteristic for the short-time regime. Motivated by the exceptional quality of cQED experiments [26–28], we thus dedicate the remainder of this Letter to the reconstruction of the FCS by coupling a qubit dispersively to the observable of interest. As discussed above, the (unperturbed) moment generating function Eq. (1) can be accessed through the off-diagonal density matrix element of a qubit which couples to the observable of interest with the coupling Hamiltonian, $\hat{H}_c = \lambda\hat{n}\hat{\sigma}_z/2$. Since the FCS is given by the Fourier transform of the moment generating function, the latter would have to be measured for all possible values of the coupling strength λ in order to faithfully reconstruct the FCS. Here we are interested in how well this reconstruction performs if the measurements are limited in number and the coupling strength cannot exceed a maximal value.

As shown in Fig. 2(b), a maximal coupling strength of $\lambda_{\max} \approx 420\kappa$ with 500 equally spaced measurement points is sufficient to reconstruct most features of the FCS. As discussed in the Supplemental Material [24], this procedure is robust against uncertainties in the coupling strength up to a magnitude of $\sim\kappa/2$. However, some care has to be taken in the choice of $\lambda_{\max}$ and the postprocessing of the measured values.

Conclusions.—By unraveling the FCS in terms of trajectories through Hilbert space, we demonstrated that negative FCS arise from a peculiar interference effect, where the interference contribution from a pair of trajectories can contribute without the corresponding classical probabilities. Our approach highlights how negative FCS are directly tied to nonclassical *dynamics*, in contrast to standard quasiprobabilities which characterize nonclassical *states*. We hope that the understanding of negative FCS presented here will inspire further work on nonclassical dynamical processes, as well as experiments to measure these effects.

We acknowledge useful comments from D. Dasenbrook, Y. Nazarov, P. Solinas, and S. Gasparinetti. This work was supported by NSERC. P. P. H. acknowledges funding from the Swiss NSF.

[1] E. Wigner, On the quantum correction for thermodynamic equilibrium, Phys. Rev. **40**, 749 (1932).
[2] *Quantum Mechanics in Phase Space: An Overview with Selected Papers*, World Scientific Series in 20th Century Physics Vol. 34, edited by C. K. Zachos, D. B. Fairlie, and T. L. Curtright (World Scientific, Singapore, 2005).
[3] M. Howard, J. Wallman, V. Veitch, and J. Emerson, Contextuality supplies the 'magic' for quantum computation, Nature (London) **510**, 351 (2014).
[4] V. Veitch, C. Ferrie, D. Gross, and J. Emerson, Negative quasi-probability as a resource for quantum computation, New J. Phys. **14**, 113011 (2012).
[5] L. S. Levitov, H. Lee, and G. B. Lesovik, Electron counting statistics and coherent states of electric current, J. Math. Phys. **37**, 4845 (1996).
[6] *Quantum Noise in Mesoscopic Physics*, edited by Y. V. Nazarov (Springer, New York, 2003).
[7] Y. V. Nazarov and M. Kindermann, Full counting statistics of a general quantum mechanical variable, Eur. Phys. J. B **35**, 413 (2003).
[8] A. A. Clerk, Full counting statistics of energy fluctuations in a driven quantum resonator, Phys. Rev. A **84**, 043824 (2011).
[9] A. Bednorz and W. Belzig, Quasiprobabilistic Interpretation of Weak Measurements in Mesoscopic Junctions, Phys. Rev. Lett. **105**, 106803 (2010).
[10] A. Bednorz, W. Belzig, and A. Nitzan, Nonclassical time correlation functions in continuous quantum measurement, New J. Phys. **14**, 013009 (2012).
[11] Y. V. Nazarov and Y. M. Blanter, *Quantum Transport: Introduction to Nanoscience* (Cambridge University Press, Cambridge, England, 2009).
[12] V. Gritsev, E. Altman, E. Demler, and A. Polkovnikov, Full quantum distribution of contrast in interference experiments between interacting one-dimensional Bose liquids, Nat. Phys. **2**, 705 (2006).
[13] P. Solinas and S. Gasparinetti, Full distribution of work done on a quantum system for arbitrary initial states, Phys. Rev. E **92**, 042150 (2015).
[14] K. Saito and A. Dhar, Fluctuation Theorem in Quantum Heat Conduction, Phys. Rev. Lett. **99**, 180601 (2007).
[15] C. Flindt and J. P. Garrahan, Trajectory Phase Transitions, Lee-Yang Zeros, and High-Order Cumulants in Full Counting Statistics, Phys. Rev. Lett. **110**, 050601 (2013).
[16] J. M. Hickey, C. Flindt, and J. P. Garrahan, Intermittency and dynamical Lee-Yang zeros of open quantum systems, Phys. Rev. E **90**, 062128 (2014).
[17] H. Wei and Y. V. Nazarov, Statistics of measurement of noncommuting quantum variables: Monitoring and purification of a qubit, Phys. Rev. B **78**, 045308 (2008).
[18] W. Belzig and Y. V. Nazarov, Full Counting Statistics of Electron Transfer between Superconductors, Phys. Rev. Lett. **87**, 197006 (2001).
[19] A. Bednorz and W. Belzig, Quasiprobabilistic Interpretation of Weak Measurements in Mesoscopic Junctions, Phys. Rev. Lett. **105**, 106803 (2010).
[20] A. A. Clerk, F. Marquardt, and J. G. E. Harris, Quantum Measurement of Phonon Shot Noise, Phys. Rev. Lett. **104**, 213603 (2010).
[21] A. Di Lorenzo and Y. V. Nazarov, Full Counting Statistics of Spin Currents, Phys. Rev. Lett. **93**, 046601 (2004).
[22] A. Di Lorenzo, G. Campagnano, and Y. V. Nazarov, Full counting statistics of noncommuting variables: The case of spin counts, Phys. Rev. B **73**, 125311 (2006).
[23] A. Bednorz and W. Belzig, Formulation of Time-Resolved Counting Statistics Based on a Positive-Operator-Valued Measure, Phys. Rev. Lett. **101**, 206803 (2008).
[24] See Supplemental Material at http://link.aps.org/supplemental/10.1103/PhysRevLett.116.013603 for the influence of additional degrees of freedom, added noise of the measurement, an explicit calculation of the FCS for an initial Fock state, and issues related to reconstructing the FCS.
[25] A. Kamenev, *Field Theory of Non-Equilibrium Systems* (Cambridge University Press, Cambridge, England, 2011).
[26] H. Paik, D. I. Schuster, L. S. Bishop, G. Kirchmair, G. Catelani, A. P. Sears, B. R. Johnson, M. J. Reagor, L. Frunzio, L. I. Glazman, S. M. Girvin, M. H. Devoret, and R. J. Schoelkopf, Observation of High Coherence in Josephson Junction Qubits Measured in a Three-Dimensional Circuit QED Architecture, Phys. Rev. Lett. **107**, 240501 (2011).
[27] A. Wallraff, D. I. Schuster, A. Blais, L. Frunzio, R.-S. Huang, J. Majer, S. Kumar, S. M. Girvin, and R. J. Schoelkopf, Strong coupling of a single photon to a superconducting qubit using circuit quantum electrodynamics, Nature (London) **431**, 162 (2004).
[28] G. Kirchmair, B. Vlastakis, Z. Leghtas, S. E. Nigg, H. Paik, E. Ginossar, M. Mirrahimi, L. Frunzio, S. M. Girvin, and R. J. Schoelkopf, Observation of quantum state collapse and revival due to the single-photon Kerr effect, Nature (London) **495**, 205 (2013).
[29] K. W. Murch, K. L. Moore, S. Gupta, and D. M. Stamper-Kurn, Observation of quantum-measurement backaction with an ultracold atomic gas, Nat. Phys. **4**, 561 (2008).
[30] S. Groblacher, K. Hammerer, M. R. Vanner, and M. Aspelmeyer, Observation of strong coupling between a micromechanical resonator and an optical cavity field, Nature (London) **460**, 724 (2009).
[31] A. A. Clerk and D. W. Utami, Using a qubit to measure photon-number statistics of a driven thermal oscillator, Phys. Rev. A **75**, 042302 (2007).
[32] H. Carmichael, *An Open Systems Approach to Quantum Optics* (Springer, New York, 1991).